Dual lateral flow optical/chemiluminescence immunosensors for the rapid detection of salivary and serum IgA in patients with COVID-19 disease

DUAL LATERAL FLOW OPTICAL/CHEMILUMINESCENCE IMMUNOSENSORS FOR THE RAPID DETECTION OF SALIVARY AND SERUM IGA IN PATIENTS WITH COVID-19 DISEASE.

Aldo Roda[1,5]*, Simone Cavalera[2], Fabio Di Nardo[2], Donato Calabria[1], Sergio Rosati[3], Patrizia Simoni[4], Barbara Colitti[3], Claudio Baggiani[2], Matilde Roda[4], Laura Anfossi[2]*

[1] Department of Chemistry G. Ciamician, University of Bologna, Italy;

[2] Department of Chemistry, University of Turin, Italy;

[3] Department of Veterinary Science, University of Turin, Italy;

[4] Department of Medical and Surgical Sciences, University of Bologna, Italy;

[5] INBB, Biostructures and Biosystems National Institute, Rome, Italy

Corresponding authors:

* Prof. Laura Anfossi, Department of Chemistry, University of Turin, Via Pietro Giuria 5, 10124, Turin (TO), Italy; e-mail: laura.anfossi@unito.it.

* Prof. Aldo Roda, Department of Chemistry "G. Ciamician", University of Bologna, Via Selmi 2, 40126 Bologna (BO), Italy; e-mail: aldo.roda@unibo.it.

Highlights

- A LFIA for the point-of-care detection of IgA specific to SARS-CoV2 in serum and saliva was developed.
- GNP and HRP-mediated optical/chemiluminescence signals were detected by a smartphone CMOS and a portable CCD, respectively
- The one-step colorimetric and two-step CL IgA-LFIA enabled the detection of anti-SARS-CoV-2 IgA in 15 minutes
- Salivary IgA were identified in four COVID-19 patients by the CL IgA-LFIA after two weeks from diagnosis

Abstract

To accurately diagnose COVID-19 infection and its time-dependent progression, the rapid, sensitive, and noninvasive determination of immunoglobulins A specific to SARS-CoV-2 (IgA) in saliva and serum is needed to complement tests that detect immunoglobulins G and M. We have developed a dual optical/chemiluminescence format of a lateral flow immunoassay (LFIA) immunosensor for IgA in serum and saliva. A recombinant nucleocapsid antigen specifically captures SARS-CoV-2 antibodies in patient specimens. A labelled anti-human IgA reveals the bound IgA fraction. A dual colorimetric and chemiluminescence detection enables the affordable and ultrasensitive determination of IgA to SARS-CoV-2. Specifically, a simple smartphone-camera-based device measures the colour signal provided by nanogold-labelled anti-human IgA. For the ultrasensitive chemiluminescence transduction, we used a contact imaging portable device based on cooled CCD, and measured the light signal resulting from the reaction of the HRP-labelled anti-human IgA with a H_2O_2/luminol/enhancers substrate. A total of 25 serum and 9 saliva samples from infected and/or recovered individuals were analysed by the colorimetric LFIA, which was sensitive and reproducible enough for the semi-quantification of IgA in subjects with a strong serological response and in the early stage of COVID-19 infection. Switching to CL detection, the same immunosensor exhibited higher detection capability, revealing the presence of salivary IgA in infected individuals . For the patients included in the study (n=4), the level of salivary IgA correlated with the time elapsed from diagnosis and with the severity of the disease. This IgA LFIA immunosensor could be useful for noninvasively monitoring early immune responses to COVID-19 and for investigating the diagnostic/prognostic utility of salivary IgA in the context of large-scale screening to assess the efficacy of SARS-CoV-2 vaccines.

Keywords: COVID-19; SARS-CoV-2; Immunoglobulin A; Saliva; Rapid serological tests; Chemiluminescence

Introduction

The SARS-CoV-2 (COVID-19) pandemic has highlighted the importance of rapid, specific, and accurate diagnostic tests in limiting the spread of infection and monitoring patients' viral load and therapy. Around 200 diagnostic tests have been developed to detect the RNA of SARS-CoV-2 (through reverse-transcriptase polymerase chain reaction, rt-PCR). Other tests work by determining antibodies specific to the virus in serum following immune response. A common format for point-of-care detection of the immune response to a virus is to measure virus-specific antibodies (IgM and IgG, or in combination) in serum using the lateral flow immunoassay (LFIA), where gold nanoparticles are used to label biospecific reagents such as secondary antibodies.

A typical antibody response to exposure to antigen involves the primary humoral immune responses typified by the appearance of IgM within the first three to five days following the exposure, followed by IgG production within the first week- (Morris and Gronowski, 2010). IgG persist after the virus is no longer detectable, indicating previous infection, while IgM are transient, so their presence is associated to a recent infection. However, the production of IgM has been reported as simultaneous, preceding or following IgG production, for COVID-19 infection. In some cases, IgM were completely absent. (Bauer, 2020) Therefore, the strategy based on the separate identification of IgM and IgG and the quantification of the IgM/IgG ratio lacks of sensitivity and is not useful in defining the phase of a SARS-CoV-2 infection (Long et al., 2020; To et al. 2020). On the other hand, physiologically, the response to a viral infection begins with the production of specific immunoglobulins secreted at the site of infection. These secretory immunoglobulins A (IgA) play an important role in the protection and homeostatic regulation of the respiratory mucosal epithelium, which separates the outside environment from the inside of the body. This primary function of IgA is referred to as "immune exclusion", a process limiting the access of microorganisms and antigens to vulnerable mucosal barriers. Conventional ELISA methods based on microtiter plates on bench-top format have accurately measured serum IgA, defining their behaviour during COVID-19 infection. These studies show that serum IgA are produced with time-dependent kinetics and in larger amounts than IgM (Dahlke et al., 2020; Yu et al., 2020), suggesting that IgA may be useful in the serological characterization of COVID-19-infected individuals and as an alternative and more reliable biomarker of early COVID-19 infection compared to IgM. In details, the production of SARS-CoV-2-specific IgA has been reported in the serum of seroconverting individuals in the first week after symptoms onset (Padoan et al., 2020; Dahlke et al., 2020), IgA appeared first (Huang et al., 2020) and were found in higher amount than IgG in the early stage of the infection (Infantino et al., 2020). Furthermore, IgA levels were correlated to severity of the disease (Huang et al., 2020). The IgA are transported in the mucus via transepithelial transport and could be present in saliva or oral fluid, where they are the main antibody isotype present (Guo et al. 2020, Ceron et al., 2020).

As a complement to IgG detection, one significant advantage of targeting IgA is the possibility of using saliva instead of blood for the analysis. Salivary anti-SARS-CoV-2 IgA have been shown to correlate with serum amounts (Randad et al., 2020). Saliva collection has several advantages over blood withdrawal,

especially for point-of-care testing (Ong et al. 2020). Saliva can be collected easily by the patient, reducing the risk associated with contact between operator and patient. Furthermore, saliva collection is particularly suitable for babies and elderly people, and for cheap population screening in low-resource settings. However, at present, there are no rapid tests for detecting SARS-CoV-2-specific IgA in saliva.

The rapid and specific detection of serum and salivary IgA could deliver early and hopefully time-dependent information about the infection. In particular, due to inconsistent findings about the evolution of IgM levels during infection, a serological marker of recovery is needed to reduce the number of rRT-PCR analyses and support decision-making about ending quarantine. Moreover, a portable easy-to-use test for serum and salivary IgA could help evaluate the individual response to therapy or vaccination against the virus in large populations.

For IgA analysis, we developed an LFIA based on a SARS-CoV-2-specific antigen (the nucleocapsid protein N), which is used as the capturing reagent and anchored onto the detection membrane. The N protein was selected among antigenic targets of the SARS coronavirus structure in a previous work of the group because it is highly immunogenic and abundantly expressed (Zeng et al., 2020) and according to its reactivity to human sera from COVID-19 patients (Cavalera et al., 2020) The optical immunosensor includes an anti-human IgA (anti-IgA) labelled with gold nanoparticles (GNP) to reveal the IgA bound to the N antigen. The anti-SARS-CoV-2 IgA in the serum/saliva sample is captured by the N antigen and stained by the GNP-labelled anti-IgA, forming a coloured band at the test line. For signal transduction and quantification of the GNP-based LFIA, we imaged the coloured strip using a smartphone camera. We reported the results in RGB scale under optimized reading conditions using the smartphone flash, as previously reported (Calabria et al., 2017). To achieve higher detectability compared to the coloured GNP probe, we used the same LFIA format, but with chemiluminescence (CL) detection mediated by a horseradish peroxidase (HRP) labelled anti-IgA and an enhanced CL luminol/H2O2/enhancer substrate (Di Nardo et al., 2016). The CL signal to noise was improved compared to the previous system by adding the CL substrate solution directly to the control and test line area after the LFIA run, thus minimizing the nonspecific light signal. The CL emitted light is measured by an ultrasensitive cooled CCD in contact imaging mode, with the data reported in relative light units.

Both immunosensor platforms allow data recording and can be used for comparative evaluation within the same patient to monitor the presence of IgA in saliva and/or serum and connect this data to disease progression and a possible decrease in viral load. The noninvasive collection of saliva is a further strength of this test. This work describes the first dual LFIA platform for the rapid detection of salivary and serum IgA and illustrates its application for SARS-CoV-2 infection.

Materials and Methods

Reagents and materials

Gold (III) chloride trihydrate (ACS reagent), mouse antihuman immunoglobulin A monoclonal antibody A (α-chain specific), protein A from Staphylococcus aureus (SpA), sucrose, and bovine serum albumin (BSA) were obtained from Merck group (Darmstadt, Germany). Tween20 and other chemicals were purchased from VWR International (Milan, Italy). Nitrocellulose membranes with cellulose adsorbent pad, blood separator, and saliva-specific sample pads were purchased from MDI Membrane Technologies (Ambala, India). Glass fiber conjugate pads were obtained from Merck Millipore (Billerica, MA, USA). HRP-labelled mouse antihuman IgA were obtained from Invitrogen, Thermo Fisher Scientific (Rockford, IL). The Supersignal ELISA Femto CL substrate for HRP was purchased from Thermo Fisher Scientific Inc. (Rockford, IL).

The IgA-LFIA strip

The LFIA strip for the colorimetric IgA-LFIA biosensor is schematized in Figure 1a. The nucleocapsid (N) antigen (1mg/ml in phosphate buffer 20 mM pH 7.4) and staphylococcal protein A (SpA, 0.5 mg/ml in phosphate buffer) were spotted at 1 µl/cm by means of a XYZ3050 platform (Biodot, Irvine, CA, USA) to form the test (TL) and control (CL) lines, respectively. The preparation of the recombinant nucleocapsid protein was previously described in Cavalera et al. (2020) and is detailed in the SI.

For the optical IgA-LFIA, gold nanoparticles (GNP) of ca. 30 nm diameter and SPR band centered at 525 nm were synthesised by tetrachloroauric reduction and conjugated to a murine anti-human IgA by passive adsorption, as previously reported (Di Nardo et al., 2017). Briefly, the anti-IgA was added to a pH-adjusted GNP solution (pH 8.5), in the proportion 10 µg per ml of GNP (optical density, OD 1). The uncovered GNP surface was saturated with BSA and the GNP-anti IgA were concentrated and recovered by centrifugation. GNP-labelled anti-IgA were pre-adsorbed in the conjugate pad (0.1 ml/cm). Sample pad, conjugate pad, the membrane, and adsorbent pad were overlapped, and strips were cut (4 mm-width). The strips were inserted into plastic cassettes.

For the chemiluminescence detection, strips were prepared as described above, except for the detection reagent (anti-human IgA-HRP, from Sigma-Aldrich), which was pre-adsorbed onto the conjugate pad as diluted 1/1000 with phosphate buffer. In addition, the membrane was saturated with 1% BSA after line deposition. In this case, the cassette was not used to maximise the contact between the strip and the CL reader.

Optical LFIA to detect IgA specific to SARS-CoV-2-

Serum and saliva were diluted by 1:10 and 1:5 v/v with Tris-glycine buffer 0.1M (pH 8, with 0.2% casein and 1% Tween 20 added), respectively. 80 µl of diluted specimen were used and LFIA results were visually inspected at 15 min from sample application. For the (semi)-quantitative evaluation of TL colour, the LFIA strip was placed in front of the back-illuminated CMOS based camera, inside the mini dark box to exclude

ambient light, and an additional lens was used to focus the T and C line image and standardize the reading using the smartphone flash illumination. A semicover and a mini dark box adaptable to any smartphones were made with 3D printing (Figure 1b). Images were then digitally processed using an RGB scale to quantify the colour. The setup of the apparatus and image processing are described in further detail in the SI.

CL-LFIA to detect IgA anti SARS-CoV-2-

For the chemiluminescence detection, we developed a simple device based on a cooled CCD camera with the LFIA strip in contact with the sensor using a fibre optic faceplate. The scheme of the device is reported in Figure 2a and further detailed in the SI. The assay was carried out in a similar way to the colorimetric assay. At 15 min from sample application, the activity of the HRP labelled antibody was measured by overlaying a transparent glass fibre pad on the detection membrane (Figure 2b). The pad contained freeze-dried sodium perborate, luminol, and p-iodophenol (Deng et al., 2016). Once in contact with the LFIA strip and following the addition of 20 µl of water, this delivered the CL substrate with production of light (Zangheri et al., 2015). The cooled CCD reader and device were placed in contact with the strip, imaged, and the CL analytical signal was quantified and expressed in relative light units (RLU).

Results and Discussion

IgA-LFIA to detect IgA specific to SARS-CoV-2 in serum

We made an optical LFIA prototype to selectively detect anti-SARS-CoV-2 IgA and verified its ability to detect the target immunoglobulins in the serum of COVID-19-infected individuals. The immunosensor included the recombinant nucleocapsid protein from SARS-CoV-2 to capture antibodies specific to the virus, and an anti-IgA labelled with GNP as the probe (Figure 1a). The test line (TL) was coloured in the presence of anti-SARS-CoV-2 IgA in the specimen because these interacted with the immobilized N antigen and were stained by the GNP probe. SpA, which captured the excess of the labelled anti-IgA used as the control line (CL) to confirm the validity of the assay. The diagnostic specificity of the IgA-LFIA was checked by analysing ten serum samples that did not contain any SARS-CoV-2-specific antibodies, as they were collected before the COVID-19 outbreak. No false positive results were recorded (false positive rate=0/10). Regarding positive samples, we analysed 25 human sera from infected individuals as confirmed by rt-PCR. Blood samples were collected at variable times from the diagnosis, and some individuals (n= 17) recovered in the meantime. Of the 25 serum samples analysed by the IgA-LFIA, 15 showed colouring of the TL and were then assigned as IgA positive. Compared to the rt-PCR method, the false negative rate was calculated as 40.0%% (10/25). Interestingly, plotting the number of IgA positive samples on the timeframe from infection diagnosis and recovery showed two clear patterns (Figure S1a in the SI). Although the number of analysed

samples is not sufficient to draw conclusions, we speculate that IgA increased during the second week of infection, peaked at the fourth week, and then declined. This trend is congruent with that reported by Padoan et al. (2020). We also observed that the IgA level in serum dramatically dropped a few days after recovery (Figure S1b in the SI).

Repeatability of the IgA-LFIA was studied by analysing, in duplicate, three serum samples classified as positive and three as negative, then calculating the mean relative standard deviation (RSD%). Stability was investigated by analysing one positive and one negative serum sample at 0, 7, and 28 days from IgA-LFIA device construction. The quantification of TL colour of positive results by the smartphone camera showed that the colorimetric IgA-LFIA provided sufficiently repeatable and stable results (RSD% for duplicate analysis of three positive samples were below 15%, and the TL intensity varied within 10% over four weeks from IgA-LFIA construction).

IgA-LFIA to detect anti-SARS-CoV-2 IgA in saliva

The prototype IgA-LFIA for serum was then adapted and optimized for use with saliva specimens. To this end, the blood separator sample pad included in the original device was replaced by a new sample pad recommended by the manufacturer for application to saliva and oral fluid specimens.

In previous studies, we demonstrated that replacing the optical detection of GNP with chemiluminescence detection of HRP as a label increased the detectability of LFIA assays by a factor of ten (Zangheri et al., 2015). We also showed that detectability could be further increased by using a more sensitive CL reader based on cooled CCD instead of the smartphone camera (Calabria et al., 2017). Therefore, we modified the IgA-LFIA to enable CL detection. Although increasing the sensitivity, the CL detection required an additional step to add the CL substrate. The flow of the CL substrate across the strip produced a strong background light, which affected the signal-to-noise ratio and largely increased the analysis time. In order to overcome these limitations, we designed a semi-integrated system in which the dried CL substrate was embedded in a glass fibre pad. The pad was layered onto the detection zone of the strip, after completion of sample run, so that the CL substrate was quickly dissolved by the wet LFIA. To help the CL substrate resuspension, we also added a drop of water. This innovative and effective strategy was adapted from Deng J. et al (2018), who set up a self-contained system, by which CL reagents were stored in dried form and were delivered directly on the detection zone by a microfluidic system aimed at revealing the enzymatic amplification of nucleic acids. Here, the addition of the CL in a very confined zone showed clear advantages over the traditional flow strategy as the CL substrate was rapidly and specifically made available for the enzymatic reaction. The background light was strongly reduced thus increasing the signal-to-noise ratio. In addition, by avoiding running the CL substrate by capillarity, the assay was accelerated, completing in 15 min instead of in over 30 min.

The IgA-LFIA prototypes were applied to analyse nine salivary samples. Eight were from four COVID-19 infected individuals and were collected at two and four weeks from rt-PCR diagnosis (Table S1 in the SI). One sample was collected in February for another study from a donor who, in that period, showed symptoms compatible with COVID-19 (cough, fever, fatigue, difficulty breathing), but without confirmation of COVID-19.

The detectability of both colorimetric and CL IgA-LFIA was sufficient to reveal salivary IgA in three out of the five subjects with good agreement between the detection methods (Figure 3a,b). In particular, the IgA-LFIA with both colour and CL detection revealed very high salivary IgA levels in subject #1, who was known to have a severe disease. Salivary IgA to SARS-CoV-2 were present at 2 and 4 weeks from diagnosis, and confirmed the tendency for levels to decrease over the time from infection observed for serum samples.

Subject #2, who reported moderate symptoms, showed IgA levels lower than #1. However, they were still detectable, especially by the ultrasensitive CL immunosensor. For subject #2, the intensity of the colour signal increased with time, while the CL detection confirmed the trend of IgA levels decreasing over time.

Subjects #3 and #4 provided results that were undetectable by colorimetric detection (a slight signal, close to the limit of detection, was shown for subject #3 only after 2 weeks from infection). In contrast, the CL detection highlighted the presence of salivary IgA in these subjects, at least in the early stage of the disease (week 2)

The improved detectability of the CL immunosensor was confirmed by the “unknown” sample. The results were at the limit of detection for colorimetric IgA-LFIA, but were clearly positive with CL detection (Figure 3c).

For the subjects with a known clinical condition, the results obtained by the IgA-LFIA correlate with severity of symptoms and also with serum IgG and IgM levels, as measured by a reference assay (Table S1 in the SI). Moreover, the new IgA-LFIA suggested that the ‘unknown’ sample belonged to a subject that was presumably infected in an early phase of the pandemic. These few data suggest that salivary IgA can be quantified using both detection strategies.

The colorimetric immunosensor coupled with the smartphone reading enabled the one-step affordable determination of IgA levels in saliva. The introduction of a simple and portable tool to quantify the color at the test line, which is related to amount of IgA, can help providing information on the severity and/or stage of the infection.

The CL detection using the portable cooled back illuminated CCD camera provided higher sensitivity and more accurate quantification compared to the smartphone BI-CMOS allowing to detect positivity in subjects with low serological response. Moreover, compared to previously reported CL-LFIA, we improved the signal-to-noise ratio by adding the CL substrate directly on the detection zone instead of flowing it across the LFIA strip. This modification of the protocol strongly reduced the light background and increasing detectability. The new protocol also halved the time required to complete the assay (15 min instead of 30

min), which is a major improvement for point-of-care testing... The combination with an optical/chemiluminescence transduction device also provides the option of connectivity for promptly communicating the patient's infection and/or recovery status.

Although IgG and IgM specific to SARS-CoV-2 have been reported to be present in saliva, as well as IgA, and can then be considered as possible markers for the non-invasive detection of the serological response to the infection (Randad et al. 2020; Isho et al., 2020), to the best of our knowledge, this is the only immunosensor for detecting salivary IgA reported to date. This is because almost all the rapid serology tests focus on serum IgM, IgG, and total immunoglobulins. However, the lack of information regarding the clinical meaning of salivary IgA measurements and the intrinsic variability of the composition of the oral fluids, which can affect the result especially in quantitative analysis, are current limitation of the method and needs further investigation. The validation of the developed IgA-LFIA by considering a larger number of samples is ongoing. Hopefully, results will be also double-checked by lab-scale tests to measure IgA (though methods for salivary IgA are still unavailable).

The availability of this rapid test may enable additional largescale studies on the significance of IgA as biomarkers of immune response to COVID-19 and the noninvasive screening to assess the efficacy of new vaccines. In the context of precision medicine, it could also support a personalized therapeutic intervention.

CRediT authorship contribution statement

Aldo Roda: Conceptualization, methodology for chemiluminescence LFIA, writing—original draft preparation. Simone Cavalera: Investigation for visual LFIA, writing— original draft preparation. Fabio Di Nardo: methodology for visual LFIA. Donato Calabria: methodology for chemiluminescence LFIA, writing—review and editing. Sergio Rosati: methodology and resource (SARS-CoV-2 recombinant nucleocapsid protein). Patrizia Simoni: methodology for chemiluminescence LFIA. Barbara Colitti: resource (ARS-CoV-2 recombinant nucleocapsid protein) Claudio Baggiani: Funding acquisition and project management. Matilde Roda: Resource (clinical samples and diagnosis). Laura Anfossi: Conceptualization, formal analysis, writing—review and editing. All authors have read and agreed to the published version of the manuscript.

Funding

This research was funded by University of Torino, Ricerca Locale grant and by INBB, Biostructures and Biosystems National Institute, Rome.

Acknowledgments

Authors thank Dr. Domenico Cosseddu from A.O. Ordine Mauriziano, Ospedale Umberto I di Torino (Turin, Italy) and Dr. Franca Fagioli from Department of Public Health and Pediatrics, Regina Margherita Children's Hospital, University of Turin (Turin, Italy) for providing serum samples and their characterization by rRT-PCR.and Grace Fox for the English style editing

Declaration of competing interest

The authors declare that they have no known competing financial interests or personal relationships that could have appeared to influence the work reported in this paper.

References

Bauer, G. , 2020, J. Med. Virol., doi.org/10.1002/jmv.26262

Calabria, D.; Caliceti, C.; Zangheri, M.; Mirasoli, M.; Simoni, P.; Roda, A., 2017. Biosens. Bioelectron. 94, 124-130

Cavalera, S.; Colitti, B.; Rosati, S.; Ferrara, G.; Bertolotti, L.; Nogarol, C.; Guiotto, C.; Cagnazzo, C.; Denina, M.; Fagioli, F.; Di Nardo, F.; Chiarello, M.; Baggiani, C.; Anfossi, L., 2020, Talanta, doi.org/10.1016/j.talanta.2020.121737

Ceron, J.J.; Lamy, E.; Martinez-Subiela, S.; Lopez-Jornet, P.; Capela e Silva, F.; Eckersall, P.D.; Tvarijonaviciute, A., 2020. J. Clin. Med. 9(5), 1491-1499

Dahlke, C.; Heidepriem, J.; Kobbe, R.; Santer, R.; Koch, T.; Fathi, A.; Ly, M.L.; Schmiedel, S.; Seeberger, P.H.; ID-UKE COVID-19 study group, Addo, M.M.; Loeffler, F.F., 2020. medRxiv. 2020

Deng, J.; Yang, M.; Wu, J.; Zhang, W.; Jiang X., 2018. Anal. Chem. 90, 9132−9137

Di Nardo, F.; Anfossi, L.; Giovannoli, C.; Passini, C.; Goftman, V.V.; Goryacheva, I.Y.; Baggiani, C., 2016. Talanta 150, 463-468

Di Nardo, F.; Baggiani, C.; Giovannoli, C.; Spano, G.; Anfossi, L., 2017. Microchim. Acta 184, 1295–1304

Guo, L.; Ren, L.; Yang, S.; Xiao, M.; Chang, D.; Yang, F.; Cruz, C.S.D.; Wang, Y.; Wu, C.; Xiao, Y.; Zhang, L.; Han, L.; Dang, S.; Xu, Y.; Yang, Q.; Xu, S.; Zhu, H.; Xu, Y.; Jin, Q.; Sharma, L.; Wang, L.; Wang J., 2020. Clin. Infect. Dis. 71(15), 778–785

Huang, Z. ; Chen, H.; Xue, M.; Huang, H.; Zheng, P.; Luo, W.; Liang, X.; Sun, B.; Zhong, N.; 2020, Clin Exp Immunol. 10.1111/cei.13500.

Infantino, M.; Manfredi, M.; Grossi, V.; Lari, B.; Fabbri, S.; Benucci, M.; Fortini, A.; Damiani, A.; Mobilia, E. M.; Panciroli, M.; Pancani, S.; Pesce, G., 2020, J Med Virol. 10.1002/jmv.26422

Isho, B.; Abe, K.; Zuo, M.; Jamal, A. J.; Rathod, B.; Wang, J. H.; Li, Z.; Chao, G.; Rojas, O. L.; Bang, Y. M.; Pu, A.; Christie-Holmes, N.; Gervais, C.; Ceccarelli, D.; Samavarchi-Tehrani, P.; Guvenc, F.; Budylowski, P.; Li, A.; Resources, A. P.; Yue, F.Y.; Marin, L.M.; Caldwell, L.; Wrana, J. L.; Colwill, K.; Sicheri, F.; Mubareka, S.; Gray-Owen, S. D.; Drews, S. J.; Siqueira,W. L.; Barrios-Rodiles, M.; Ostrowski, M.; Rini, J. M.; Durocher, Y.; McGeer, A. J.; Gommerman, J. L.; Gingras, A-C., 2020, Sci. Immunol. 5 (52) eabe5511

Li, C.; Zhao, C.; Bao, J.; Tang, B.; Wang, Y.; and Gu, B., 2020. Clin. Chim. Acta. 510, 35-46

Long, QY.; Liu, B.Z.; Deng, H.J.; Wu, G.C.; Deng, K.; Chen, Y.K.; Liao, P.; Qiu, J.F.; Lin, Y.; Cai, X.F.; Wang, D.Q.; Hu, Y.; Ren, J.H.; Tang, N.; Xu, Y.Y.; Yu, L.H.; Mo, Z., Gong, F.; Zhang, X.L.; Tian, W.G., Hu, L.; Zhang, X.X.; Xiang, J.L.; Du, H.X.; Liu, H.W.; Lang, C-H.; Luo, X.H.; Wu, S.B.; Cui, X.P.; Zhou, Z.; Zhu, M.M.; Wang, J.; Xue, C.J.; Li, X.F.; Wang, L.; Li, Z.J.; Wang, K.; Niu, C.C.; Yang, Q.J.; Tang, X.J.; Zhang, Y., Liu, X.M.; Li, J.J.; Zhang, D.C.; Zhang, F.; Liu, P.; Yuan, J.; Li, Q.; Hu, J.L.; Chen, J.; and Huang, A.L., 2020. Nat Med. 26, 845–848

Morris, G.P.; and Gronowski, A.M., 2010, Laboratory approaches to serology testing In: Clinical Chmistry Theory Analysis Correlation, 5th ed. Kaplan L.A. Pesce A.J Eds, Mosby, Inc, (USA)

Ong, D.S.Y.; de Man, S.J.; Lindeboom, F.A.; Koeleman, J.G.M., 2020. Clin. Microbiol. Infect. 26, 1094.e7-1094.e10

Padoan, A.; Sciacovelli, L.; Basso, D.; Negrini, D.; Zuin, S.; Cosma, C.; Faggian, D.; Matricardi, P.; Plebani, P., 2020. Clin. Chim. Acta. 507, 164-166

Randad, P.R.; Pisanic, N.; Kruczynski, K.; Manabe, Y.C.; Thomas, D.; Pekosz, A.; Klein, S.L.; Betenbaugh, M.J.; Clarke, W.A.; Laeyendecker, O.; Caturegli, P.P.; Larman, H.B.; Detrick, B.; Fairley, J.K.; Sherman, A.C.; Rouphael, N.; Edupuganti, S.; Granger, D.A.; Granger, S.W.; Collins, M.; Heaney, C.D., 2020. medRxiv. 2020

To, K.K.W.; Tsang, O.T.Y.; Leung, W.S.; Tam, A.R.; Wu, T.C.; Lung, D.C.; Yip, C.C.Y.; Cai, J.P.; Chan, J.M.C.; Chik, T.S.H.; Lau, D.P.L.; Choi, C.Y.C.; Chen, L.L.; Chan, W.M.; Chan, K.H.; Ip, J.D.; Ng, A.C.K.; Poon, R.W.S.; Luo, C.T.; Cheng, V.C.C.; Chan, J.F.W.; Hung, I.F.N.; Chen, Z.; Chen, H.; Yuen, K.Y., 2020. Lancet Infect Dis. 20, 565–74

Yu, H.Q.; Sun, B.Q.; Fang, Z.F.; Zhao, J.C.; Liu, X.Y.; Li, Y.M.; Sun, X.Z.; Liang, H.F.; Zhong, B.; Huang, Z.F.; Zheng, P.Y.; Tian, L.F.; Qu, H.Q.; Liu, D.C.; Wang, E.Y.; Xiao, X.J.; Li, S.Y.; Ye, F.; Guan, L.; Hu, D.S.; Hakonarson, H.; Liu, Z.G.; Zhong, N.S., 2020. Eur. Respir. J. 2020

Zangheri, M.; Cevenini, L.; Anfossi, L.; Baggiani, C.; Simoni, P.; Di Nardo, F.; Roda, A., 2015. Biosens. Bioelectron. 64, 63-68

Zeng, W.; Liu, G.; Ma, H.; Zhao, D.; Yang, Y.; Liu, M.; Mohammed, A.; Zhao, C.; Yang, Y.; Xie, J.; Ding, C.; Ma, X.; Weng, J.; Gao, Y.; He, H.; Jina, T., 2020. Biochem. Biophys. Res. Commun. 527(3), 618–623

Figure captions

Figure 1. Scheme of: (a) the LFIA strip to detect anti-SARS-CoV-2 IgA. The serum or salivary sample is applied to the sample pad and flows longitudinally by capillarity, resuspends the probe (GNP or HRP-labelled anti human IgA), and the mix flows through the detection membrane where it encounters the nucleocapsid protein (N) on the test line (TL) and the staphylococcal protein A (SpA) on the control line (CL). Anti-SARS-CoV-2 IgA in the sample are selectively captured at the TL and stained by the probe. The CL captures the probe, regardless of the presence of the target immunoglobulins in the sample. b) the smartphone reader used for the optical immunosensor.

Figure 2. a) Scheme of the CCD camera, and b) protocol for the ultra-high sensitivity CL detection of salivary IgA by the developed immunosensor. After completion of the IgA-LFIA (1), a transparent glass fibre pad (which was pre-impregnated with the CL cocktail substrate) is placed onto the membrane at the test and control line (2). 20 µl of water is added to assist the re-suspension of the CL substrate; finally, the strip is placed in the holder of the cooled CCD camera for lens-free imaging detection (3).

Figure 3. IgA-Anti-SARS-CoV-2 detection in saliva from four donors as detected by the colorimetric (a) and chemiluminescent (b) IgA-LFIA sensor. A salivary sample collected in Italy before the outbreak of the pandemic from an individual with symptoms compatible with those of COVID-19 was shown to contain apparent anti-SARS-CoV-2 IgA by the IgA-LFIA (c). Data are shown as the mean ± std dev of two replicate measurements.

Figures

Figure 1

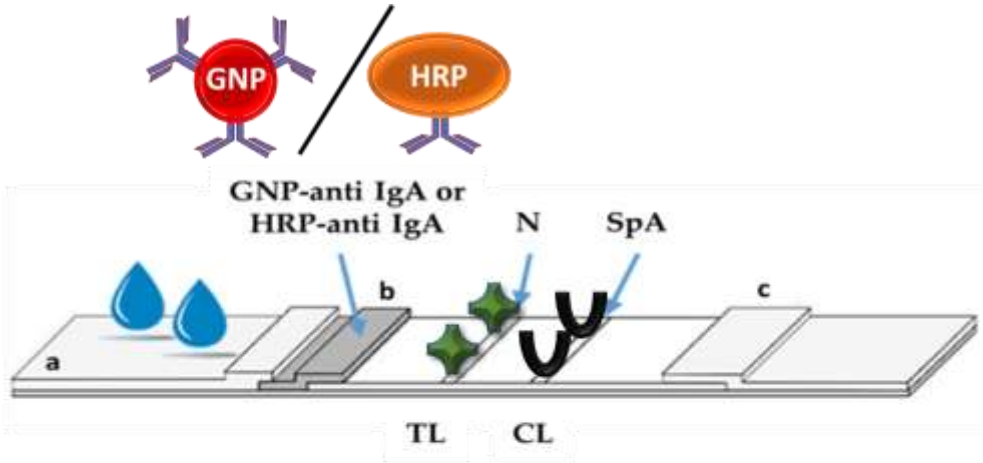

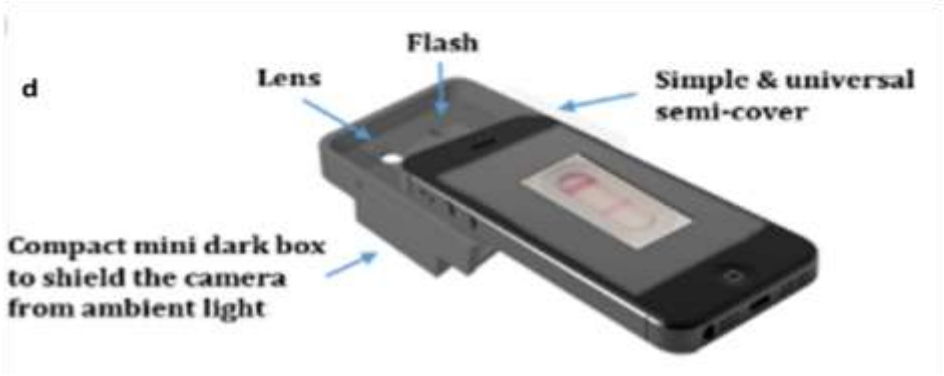

Figure 2

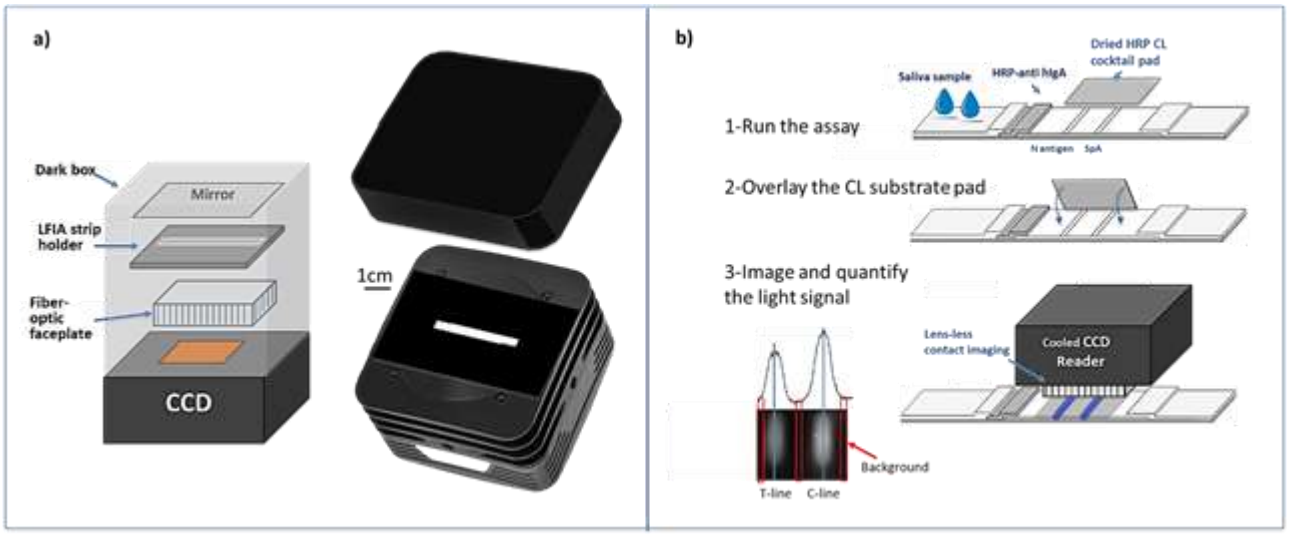

Figure 3

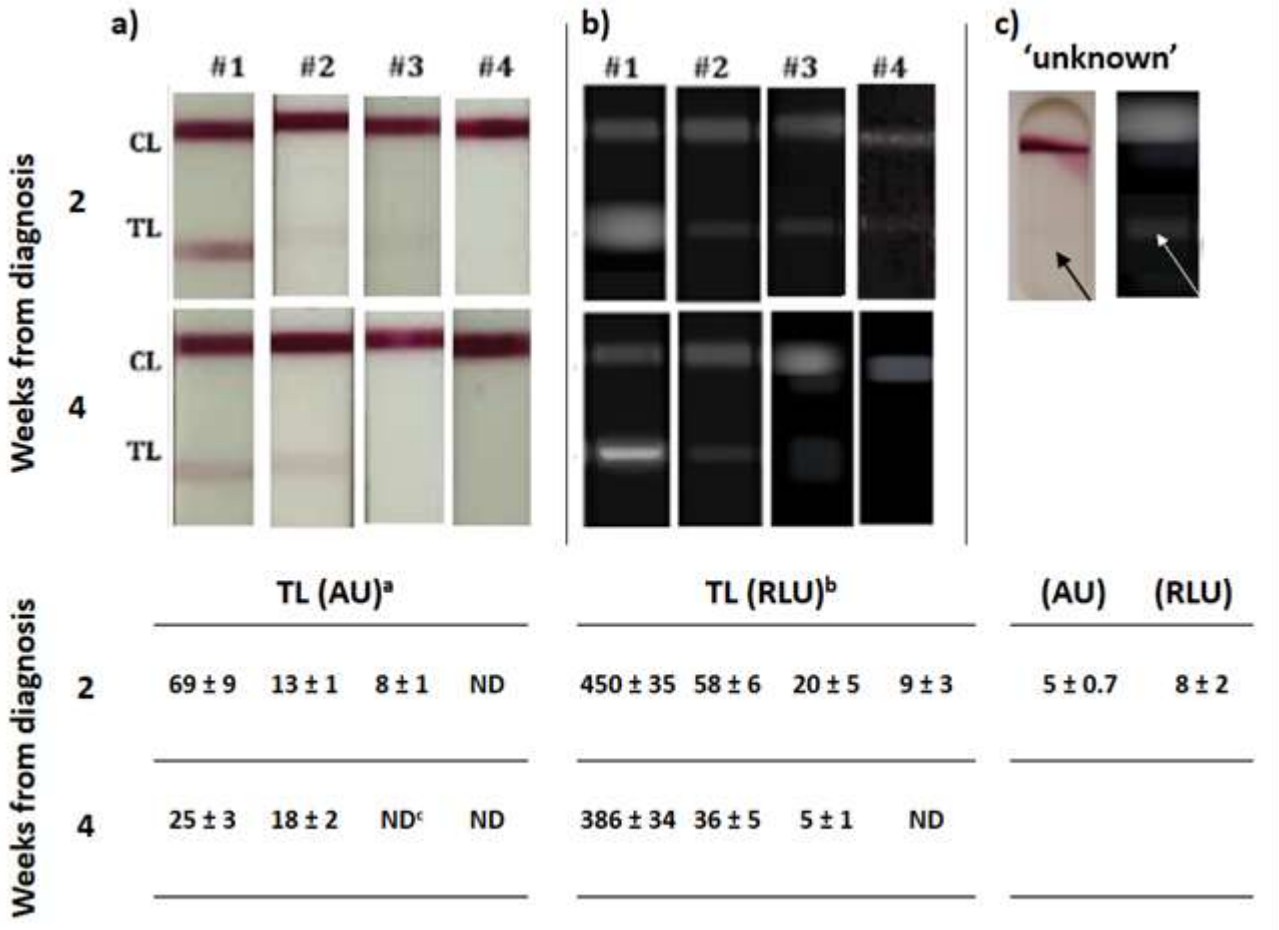

Weeks from diagnosis	TL (AU)[a]				TL (RLU)[b]				(AU)	(RLU)
2	69 ± 9	13 ± 1	8 ± 1	ND	450 ± 35	58 ± 6	20 ± 5	9 ± 3	5 ± 0.7	8 ± 2
4	25 ± 3	18 ± 2	ND[c]	ND	386 ± 34	36 ± 5	5 ± 1	ND		

[a] arbitrary units as measured by the smartphone reader, [b] relative lights units as measured by CCD camera, [c] not detectable (threshold:mean background signal + 2 standard deviation)

Supporting Information

Content

1. Experimental section

Production of the recombinant SARS CoV-2 nucleocapsid protein

The N recombinant antigen was successfully expressed as partially soluble protein. Purification was achieved under mild denaturing condition (1M urea fraction) and evaluated by SDS-PAGE, showing a single protein band of molecular weight corresponding to the expected size. Sequence analysis of each of two bacterial clones confirmed the identity and correct orientation of the insert.

Smartphone color reader

Any smartphone with a back-illuminated CMOS (e.g. iPhone X) can be used. A 3D-printed semicover frame allows it to be fixed to the reader. The target area corresponding to the test and control line of the LFIA membrane strip was uniformly illuminated by adding a PDMS light diffuser in the dark box (40 × 40 × 60 mm) placed in front of the smartphone flash. The focal distance of the smartphone camera has been reduced to ∼ 10 mm by adding a 0.4X wide-angle two-lenses optical element with a 140° viewing angle. The dark box avoids interference from ambient light. The smartphone holder con be ad-hoc designed according to the smartphone model to ensure correct positioning of the smartphone camera and flash. The dark box is then connected to the lab-case and the smartphone is inserted in the holder. 15 minutes upon delivering the sample on the LFIA strip, the image is acquired with the dedicated app Camera FV-5 Lite using the following acquisition parameters: ISO 800, time exposure 0.1 s, flash on. The image is saved in TIFF format and then quantitative image analysis is performed using the freeware software ImageJ v.1.46. For each image, a region of interest (ROI) corresponding to the sample chamber containing the test and control lines of the LFIA membrane was selected, then the RGB values were computed and converted to HSV. The Saturation (S) value of HSV color space obtained from the image acquired in a different area of the membrane (background signal) was then subtracted from the S value obtained 60 s after sample application, to obtain a corrected S value.

CCD device for CL imaging

A commercially available CCD camera (ATIK 11000, ATIK Cameras, New Road, Norwich) equipped with a large format, high resolution monochrome CCD sensor (Kodak KAI 11002, sensor size 37.25 × 25.70 mm)

cooled by a two-stage Peltier element to reduce thermal noise was used as CL signal reader. The CCD camera was modified by replacing its upper part (i.e., the CCD sensor compartment and the optical glass window) with an aluminum cartridge housing assembly, which ensures the correct alignment of the CCD sensor with the LFIA strip during the measurement and avoids interference from ambient light. The cartridge housing assembly is composed by the strip holder and a lower fixing plate. The inner cavity of the strip holder fits the dimensions of the LFIA cartridge and ensures the close contact between the LFIA cartridge and the fiber optic faceplate. The fiber optic faceplate (size 26 × 26 × 13 mm, Edmund Optics, Barrington, NJ) is fabricated in polymethylmethacrylate (PMMA) and conveys the CL signal from the LFIA strip to the CCD sensor. Inside the upper surface of the dark box is inserted a mirror to ensure the complete and total collection of the light, increasing the sensitivity of the measurement. The CL reader is connected to a laptop via an USB interface. The ImageJ software was used also for CL signal elaboration. The mean photon emission of the C-line and T-line of the LFIA strip was measured and corrected for the mean background signal measured in adjacent areas expressed in CL intensity in arbitrary units.

Serum and Saliva samples

Ten negative human serum samples (collected before the SARS CoV-2 outbreak) and twenty-five positive human serum samples were collected within the SIRIT project.

Positive human sera were selected according to: i) having a positive rRT-PCR analysis on a swab sample, ii) having been assigned as positive for anti-SARS-CoV-2 IgG by a validated ELISA serological kit (ERADIKITTM COVID19-IgG).

Blood samples were collected by venipuncture at variable times from the rRT-PCR diagnosis. Serum was immediately obtained from blood and stored at -20°C until analysis. Some individuals (n= 17) recovered in the meantime (according to the rRT-PCR negative). Saliva samples were collected by means of the SalivaBio Oral Swab (Salimetrics, CA, USA), immediately refrigerated, and stored for at least 24 h at 20 °C before centrifugation and analysis.

Four volunteers provided saliva samples. They were members of a COVID-19 infected family, including father, mother, and two sons (38 and 42 years old). They provided saliva after 2 and 4 weeks from diagnosis by rt-PCR.

Subject #1, male, age 71, was affected by severe symptoms, with typical COVID-19 clinical manifestation and chest radiology. He was hospitalized in an intensive care unit for 10 days, and then clinically recovered after 4 weeks.

Subject #2, female, age 64, wife of #1, was affect by moderate/mild symptoms and did not require hospitalization. After 3 weeks from diagnosis fully recovered.

Subjects #3, age 35 male, and Subject #4, age 43 male, brothers and sons of #1 and #2 where asymptomatic or with only slight fatigue and caught manifestation.

Subjects 1-4 were also tested by a serological assay for the content of IgM and IgG in serum, at two weeks from diagnosis (Table S1).

The saliva of an additional subject, called ‘unknown’, male, age 30, was available in the la, as it was collected on February 2019, before COVID-19 outbreak, for another study. The subject had shown clinical manifestation attributable to the SARS-CoV-2 infection, but recovered before the outbreak and was not submitted to rt-PCR testing.

All donors provided informed consent to the use of their specimens. Donors of specimen collected before the outbreak were contacted and were requested to provide informed consensus for this study.

2. Figures

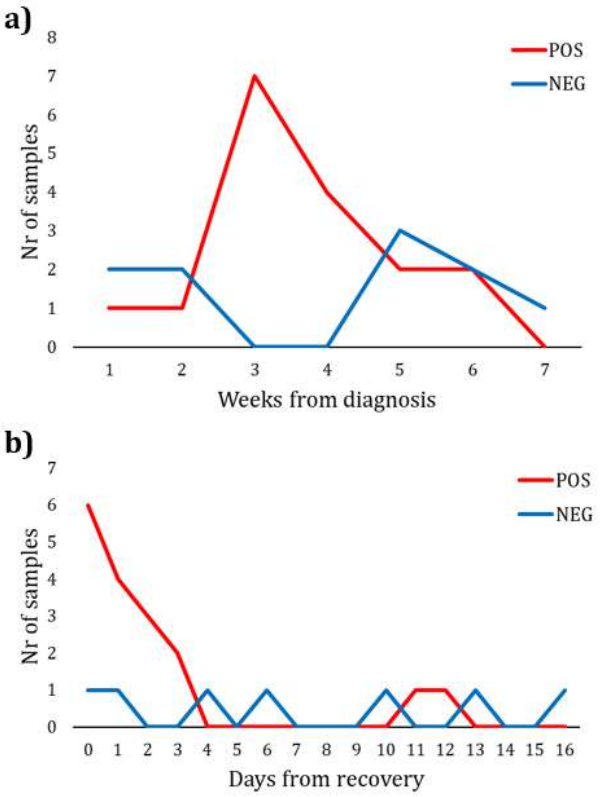

Figure S1. Results obtained from the optical immunosensor for the serum IgA specific to SARS-CoV-2 as a function of time from infection (a) and recovery (b) diagnosis.

3. Tables

Table S1. Salivary anti-SARS-CoV-2 IgA measured by the colorimetric and chemiluminescence IgA-LFIA immunosensor in four subjects affected by Covid-19 infection after 2 and 4 weeks from the diagnosis. Salivary IgA data were compared with serum anti-SARS-CoV-2 IgG and IgM as evaluated by a commercial colorimetric rapid test (KHB Covid-19 antibody from Techno Genetics).

Subject	Weeks from diagnosis	Salivary IgA (RLU)[a]	Salivary IgA (AU)[b]	Serum IgG	Serum IgM
#1	2	450 ± 35	69 ± 9	POS ++	POS +
	4	386 ± 34	25 ± 3	POS +++	POS ++

#2	2	58 ± 6	13 ± 1	POS +++	POS ++
	4	36 ± 5	18 ± 2	POS +++	POS +
#3	2	20 ± 5	8 ± 1	NA[c]	NA
	4	5 ± 1	ND	POS +++	NEG
#4	2	9 ± 3	ND	NA	NA
	4	ND[d]	ND	POS++	NEG

[a] RLU: relative light units; [b]AU arbitrary units; [c] NA: not available; [d] ND: below detectability (threshold: mean background signal + 2 standard deviation)